

Full Length Research Paper

Wet chemical synthesis of Tin Sulfide nanoparticles and its characterization

S. Suresh

Crystal Growth Centre, Anna University, Chennai-25, India.

Received 17 June, 2014; Accepted 8 September, 2014

Nanostructured materials have attracted much attention in various fields of science and technology. Tin sulfide (SnS) nanoparticles were successfully synthesized by wet chemical method. The as-prepared tin sulfide nanoparticles were characterized by X-ray diffraction, scanning electron microscopy (SEM), transmission electron microscopy (TEM) and dielectric studies. The SEM measurements show the aggregates of small nanoparticles. TEM images showed the presence of spherical tin sulfide nanoparticles of size in the range of 15 nm. The optical properties were obtained from UV-VIS absorption spectrum and the optical band gap was calculated. The dielectric constant calculated by varying the frequencies at different temperatures.

Key words: Preparation, SnS nanoparticles, scanning electron microscopy (SEM), transmission electron microscopy (TEM), optical property and dielectric constant.

INTRODUCTION

The consumption of fossil fuels has increased immensely in the recent years which made the role of renewable energy sources relevant. The other forms of energy such as coal, oil and gas are at the stage of extinction because of the extensive usage. Among the alternative energy sources, photovoltaics is known to be an almost maintenance free clean energy technology. In recent years, semiconductor nanostructures such as nanoparticles, nanorods, nanotubes, nanowires and nanobelts have attracted intensive interest due to their novel physiochemical properties that differ greatly from their bulk counterparts (Alivisatos et al., 1991). IV-VI semiconductor compounds such as PbSe, SnSe and SnS have been important role in different areas of materials science for several decades (Unger et al., 1986).

Nanomaterials were widely studied due to their unique physical and chemical properties and also its potential applications in different areas (Simon et al., 1998). These properties and potential applications have stimulated the search for new synthetic techniques for these materials. In recent years, great resources were devoted to the preparation of nanocrystals using a wide variety of methods including electrodeposition (Natter et al., 1998), solvothermal route (Zhang et al., 2003), thermal decomposition (Nayral et al., 1999) and chemical reduction (Yang et al., 2000). These efforts have led to the successful synthesis of many nanocrystals including metals (Shafi et al., 1998) oxides (Liu et al., 2001; Haubold et al., 2001), as well as sulfides (Price et al., 2000) which have already been used as optoelectronic

E-mail: drsureshphysics@gmail.com

Author(s) agree that this article remain permanently open access under the terms of the [Creative Commons Attribution License 4.0 International License](https://creativecommons.org/licenses/by/4.0/)

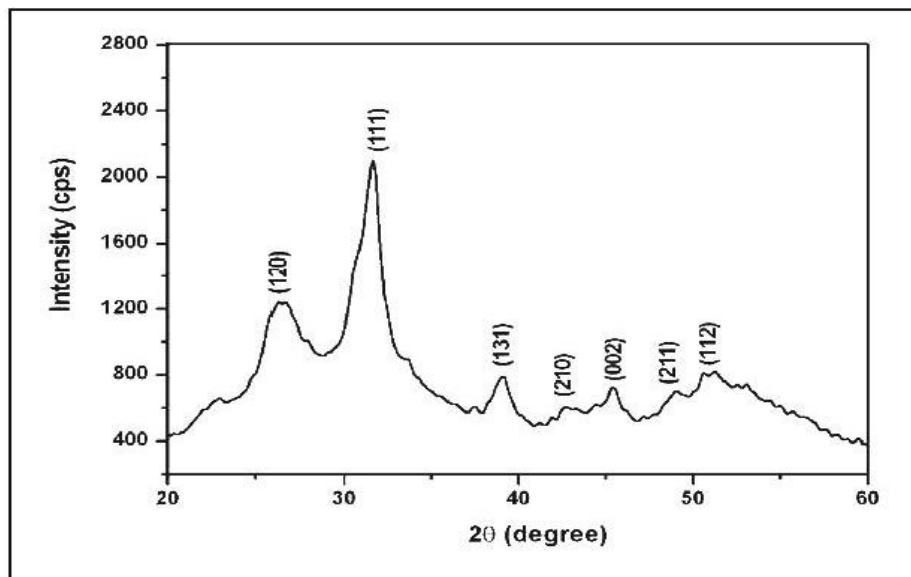


Figure 1. XRD pattern of tin sulfide nanoparticles.

materials in sensors, laser materials, solar cells and other devices. In this paper, we report a wet chemical method to prepare tin sulfide nanoparticles. Powder X-ray diffraction (XRD), scanning electron microscopy (SEM) and transmission electron microscopy (TEM) show the formation of tin sulfide nanoparticles possessing orthorhombic structure. The as-prepared tin sulfide nanoparticles display blue-UV emission, promising for applications in optical devices. Dielectric constant studies are carried out at different temperatures.

SYNTHESES OF TIN SULFIDE NANOPARTICLES

The tin sulfide nanoparticles were synthesized through wet chemical method. Tin (II) chloride ($\text{SnCl}_2 \cdot 2\text{H}_2\text{O}$) and sodium sulfide (Na_2S) were taken as tin and sulfur sources respectively and deionized water was used as solvent. 1.2 g of tin (II) chloride and 1.72 g of sodium sulfide were dissolved in deionized water. Sodium sulfide solution was added drop wise into the solution. The colorless tin (II) chloride solution turns dark brown color with the addition of sodium sulfide solution. This indicates the formation of SnS nanoparticles. This reaction was carried out at room temperature for two hours. The precipitates were centrifuged and washed with deionized water and ethanol for several times and dried at room temperature.

RESULTS AND DISCUSSION

Structural studies

XRD is a non-destructive analytical method which identifies and determines various crystalline forms of materials. According to studies, the solution of nanoparticles obtained was purified by repeated

centrifugation at 10,000 rpm followed by re-dispersion of the pellet of nanoparticles into distilled water. After freeze drying of the purified particles, the structure and composition of nanoparticles were analyzed by XRD. As waves interact with a regular structure the diffraction occurs. Figure 1 shows the XRD pattern of tin sulfide nanoparticles. All the diffraction peaks are indexed to pure orthorhombic phase of tin sulfide. This is due to agglomeration of the particles in the powdered sample and hence, XRD was used for phase identification only. The strong and sharp diffraction peaks indicate that the product is well crystallized. Phase purity is confirmed from powder X-ray diffraction. No other impurity peaks are observed. The broadening of the peaks indicates the nanocrystalline nature of SnS. By knowing the wavelength (λ) full width at half maximum (FWHM) of the peaks β and the diffracting angle θ , particle size (D) was calculated by using the Scherrer formula,

$$D = \frac{0.9\lambda}{\beta \cos \theta} \quad (1)$$

The average grain size of SnS is determined using Scherrer relation and it was found to be around 15 nm.

Optical studies

Optical absorption measurement was carried out on tin sulfide nanoparticles. Figure 2 shows the variation of the optical absorbance with the wavelength of the as-prepared tin sulfide nanoparticles. The optical absorption coefficient has been calculated in the wavelength range

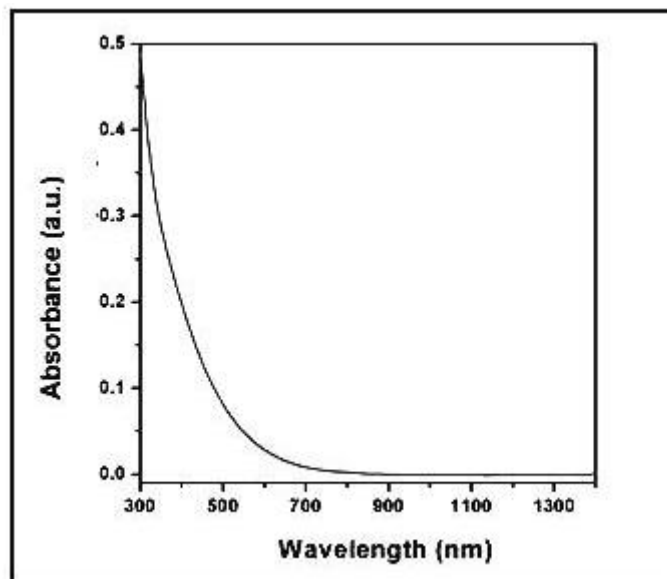


Figure 2. Optical absorption spectrum of SnS nanoparticles.

of 300 to 900 nm. It is clearly observed that the nanoparticles have a wide absorption range from the NIR to the UV, which means it is good for absorption of the sunlight. The absorption edge has been obtained at a shorter wavelength. The band gap energy gap was estimated from the Equation (1)

$$E_g = 1.243 \times 10^3 / \lambda_{max} \quad (2)$$

The band gap of tin sulfide nanoparticles was found to be 1.8 eV. In semiconductor nanoparticles, the band gap increases as the particle size decreases.

Scanning electron microscopy (SEM) analysis

External morphology, chemical composition, crystalline structure and orientation of materials making up the sample are revealed by SEM. Figure 3 shows the SEM image of tin sulfide nanoparticles. This SEM image reveals that the particles are in aggregation state due to their extremely small dimensions and high surface energy. It can be seen that the particles adopt irregular morphology with different sized particle. From the image it is clear that the particles were highly agglomerated in nature. This might be due to the fact that the agglomeration may be induced during the crystal growth itself because of the small size regime which is evident from the XRD analysis.

Transmission electron microscopy (TEM) analysis

TEM is commonly used for imaging and analytical

characterization of the nanoparticles to assess the shape, size, and morphology. The particle size distribution was also measured from the bright-field TEM image shown in Figure 4. The detection and measurement of the nanoparticles (segmentation) on this type of samples is difficult because thickness changes locally and diffraction from different crystal orientations introduce large contrast variations. Size of tin sulfide nanoparticles measured from TEM image is 15 nm.

Dielectric constant studies

Dielectric studies show the effects of temperature and frequency on the conduction phenomenon in nanostructured materials. Dielectric behavior can effectively be used to study the electrical properties of the grain boundaries. The dielectric properties of materials are mainly due to contributions from the electronic, ionic, dipolar and space charge polarizations. Among these, the most important contribution to the polycrystalline materials in bulk form is from the electronic polarization, present in the optical range of frequencies. The next contribution is from ionic polarization, which arises due to the relative displacement of the positive and negative ions. Dipolar or orientation polarization arises from molecules having a permanent electric dipole moment that can change its orientation when an electric field is applied. Space charge polarization arises from molecules having a permanent electric dipole moment that can change its orientation when an electric field is applied. The dielectric parameters, like the dielectric constant (ϵ_r) is the basic electrical properties of the tin sulfide nanoparticles. The measurement of the dielectric

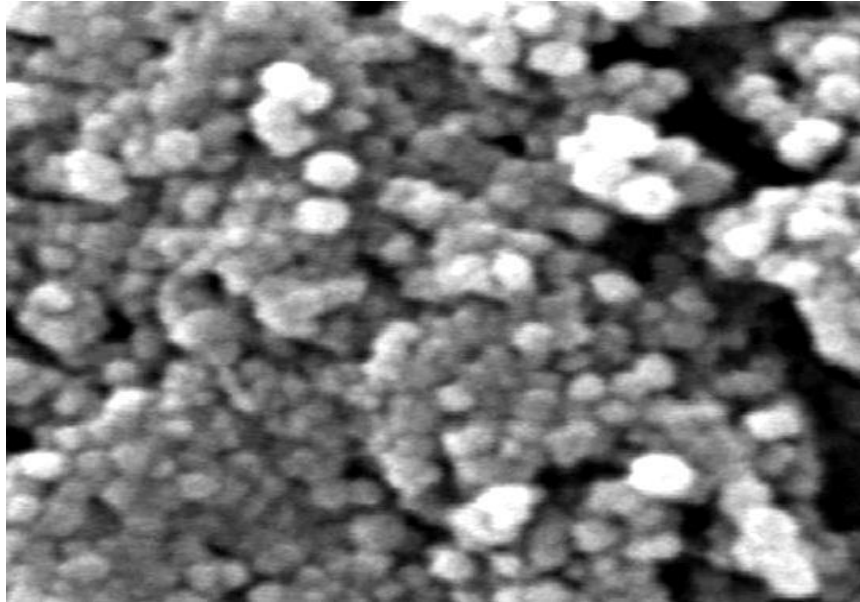


Figure 3. SEM image of tin sulfide nanoparticles.

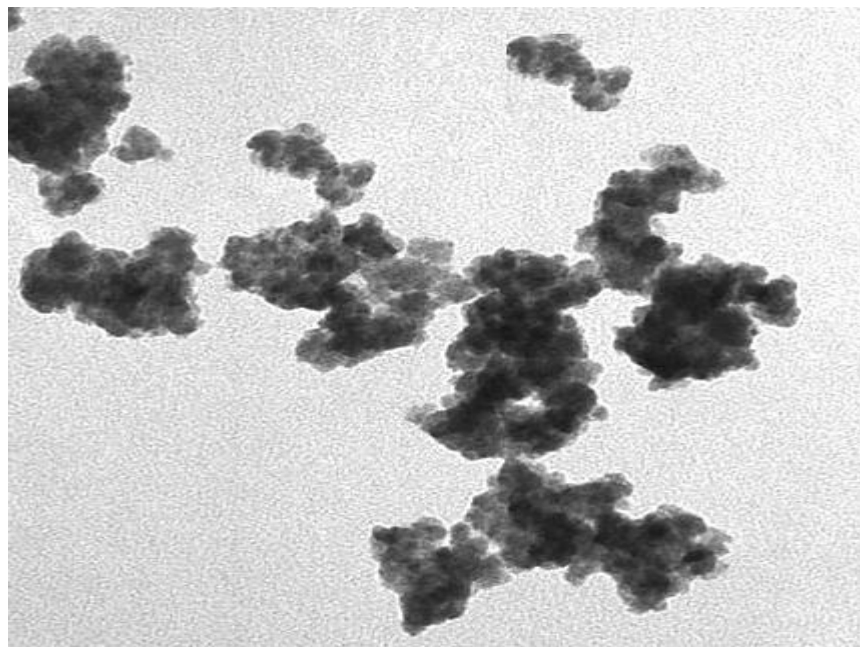


Figure 4. Typical TEM image of tin sulfide nanoparticles.

constant as a function of frequency and different temperatures reveals the electrical processes that take place in tin sulfide nanoparticles and these parameters have been measured. The variations of the dielectric constant of the tin sulfide nanoparticles at frequencies of 50Hz to 5 MHz and at different temperatures of 40, 50, 100 and 120°C are displayed in Figure 5. The dielectric constant is evaluated using the relation:

$$\epsilon_r = \frac{Cd}{\epsilon_0 A} \quad (3)$$

Where d is the thickness of the sample and A , is the area of the sample. The results suggest that the dielectric constant strongly depend on the frequency of the a.c. signal and the different temperatures of the tin sulfide

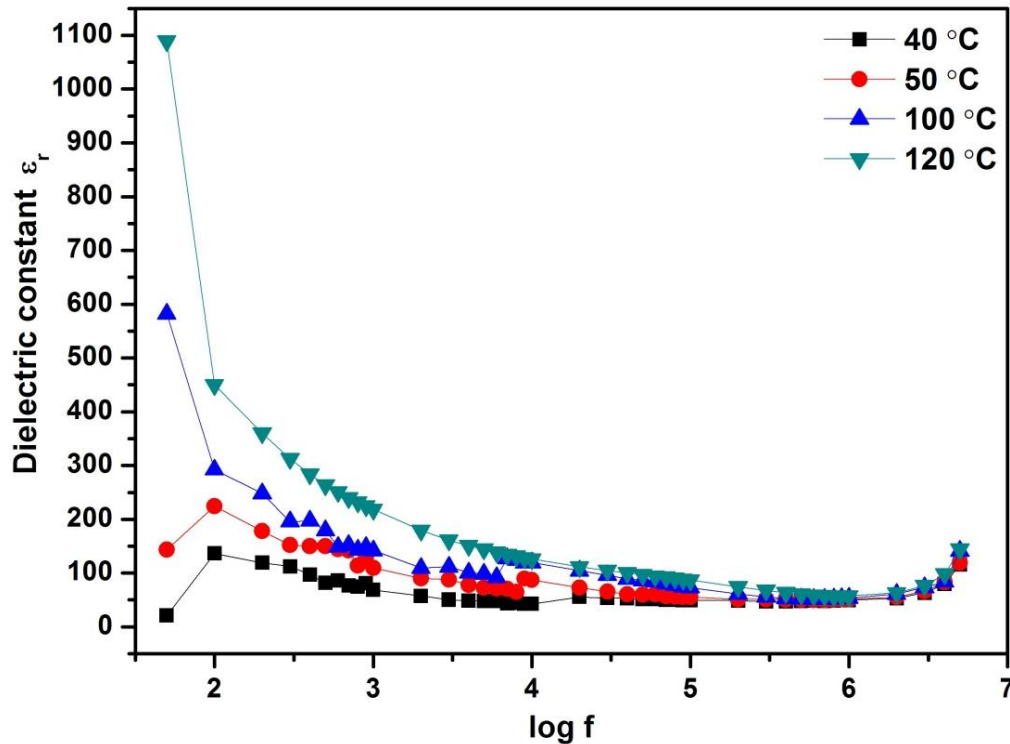


Figure 5. Variation of dielectric constant with log frequency.

nanoparticles. The dielectric constant has higher values in the lower-frequency (50 Hz) and then it decreases up to the high frequency (5 MHz). The dielectric constant of is high at lower frequencies due to the contribution of the electronic, ionic, dipolar and space charge polarizations, which depend on the frequencies (Xue et al., 2002). Space charge polarization is generally active at lower frequencies and indicates the purity and perfection of the nanoparticles. Its influence is strong at higher temperature and is noticeable in the low frequency range (Smyth et al., 1956).

The Figure 5 shows the variation of dielectric constant as function of frequency and temperatures. It is clear from Figure 5 that dielectric constant increases with the increase in temperature. This increase in dielectric constant as a result of increase in temperature can be explained on the basis of phenomenon that as the temperature increases, the dipoles relatively become free and they respond to the applied electric filed. Consequently the polarization increased and hence dielectric constant also increases with the increase in temperature. The variation of dielectric constant with frequency may be explained on the basis of space-charge polarization phenomenon (Rezlescu et al., 1974). According to this, dielectric material has well conducting grains separated by highly resistive grain boundaries. On the application of electric field, space charge accumulates at the grain boundaries and voltage drops

mainly at grain boundaries (Gul et al., 2010).

Most of the atoms in the nanocrystalline materials reside in the grain boundaries, which become electrically active as a result of charge trapping. The dipole moment can easily follow the changes in the electric field, especially at low frequencies. Hence, the contributions to the dielectric constant increase through space charge and rotation polarizations, which occur mainly in the interfaces. Therefore, the dielectric constant of nanostructured materials should be larger than that of the conventional materials. One of the reasons for the large dielectric constant of nanocrystalline materials at sufficiently high temperature is the increased space charge polarization due to the structure of their grain boundary interfaces. As the temperature increases, the space charge and ion jump polarization decrease, resulting in a decrease in the dielectric constant.

CONCLUSION

The tin sulfide nanoparticles were synthesized through wet chemical method. The XRD pattern revealed the orthorhombic structure of tin sulfide nanoparticles. SEM micrograph shows the aggregation state of tin sulfide nanoparticles. TEM images showed the presence of spherical tin sulfide nanoparticles of size in the range of 15 nm. In UV-VIS absorption spectrum shows that the

nanoparticles have a wide absorption range and 1.8 eV direct allowed transition energy gap. The as-prepared tin sulfide nanoparticles have good crystalline and show strong blue-UV emission, promising for applications in optical devices. The dielectric property studied at different temperatures.

Conflict of Interest

The authors have not declared any conflict of interest.

REFERENCES

- Alivisatos AP (1996). Semiconductor clusters, nanocrystals and quantum dots. *Science* 271: 933. <http://dx.doi.org/10.1126/science.271.5251.933>
- Gul H, Maqsood A, Naeem M, Naeem AM (2010). Optical, magnetic and electrical investigation of cobalt ferrite nanoparticles synthesized by co-precipitation route. *J. Alloys. Compd.* pp. 507,201. <http://dx.doi.org/10.1016/j.jallcom.2010.07.155>
- Haubold S, Haase M, Kornowski A, Weller H (2001). Strongly Luminescent InP/ZnS Core-Shell Nanoparticles. *Chem. Phys. Chem.* 2:331 [http://dx.doi.org/10.1002/1439-7641\(20010518\)2:5<331::AID-CPHC331>3.0.CO;2-0](http://dx.doi.org/10.1002/1439-7641(20010518)2:5<331::AID-CPHC331>3.0.CO;2-0)
- Unger K, Verbindungshalbletler A, Verlagsanstalt L (1986). *AkademischeVerlagsanstalt, Leipzig*, 339.PMCid: PMC460295.
- Liu Y, Zheng C, Wang W, Yin C, Wang G (2001). Synthesis and Characterization of Rutile SnO₂ Nanorods. *Adv. Mater.* 13:1883 [http://dx.doi.org/10.1002/1521-4095\(200112\)13:24<1883::AID-ADMA1883>3.0.CO;2-Q](http://dx.doi.org/10.1002/1521-4095(200112)13:24<1883::AID-ADMA1883>3.0.CO;2-Q)
- Natter H, Schmelzer M, Hempelmann R (1998). Nanocrystalline nickel and nickel-copper alloys: Synthesis, characterization, and thermal stability. *J. Mater. Res.* 13:1186 <http://dx.doi.org/10.1557/JMR.1998.0169>
- Nayral C, Ould-Ely T, Maisonnat A, Chaudret B, Fau P, Lescouzeres L, Peyre-Lavigne A (1999). A Novel Mechanism for the Synthesis of Tin /Tin Oxide Nanoparticles of Low Size Dispersion and of Nanostructured SnO₂ for the Sensitive Layers of Gas Sensors. *Adv. Mater.* 11:61. [http://dx.doi.org/10.1002/\(SICI\)1521-4095\(199901\)11:1<61::AID-ADMA61>3.0.CO;2-U](http://dx.doi.org/10.1002/(SICI)1521-4095(199901)11:1<61::AID-ADMA61>3.0.CO;2-U)
- Price LS, Parkin IP, Field MN, Hardy AME, Clark RJH, Hibbert TG, Molloy KC (2000). Atmospheric pressure chemical vapour deposition of tin (II) sulfide films on glass substrates from Buⁿ₃SnO₂CCF₃ with hydrogen sulfide. *J. Mater. Chem.* 10:527. <http://dx.doi.org/10.1039/a907939d>
- Rezlescu N, Rezlescu E (1974). Dielectric properties of copper containing ferrites. *Physics Status Solid A*, 23:575 <http://dx.doi.org/10.1002/pssa.2210230229>
- Shafi KYPM, Gedanken A, Prozorov R (1998). Sonochemical preparation and characterization of nanosized amorphous Co-Ni alloy powders. *J. Mater. Chem.* 8:769 <http://dx.doi.org/10.1039/a706871i>
- Smyth CP (1956). Dielectric behavior and structure. *Acta Cryst* 9:838-839. <http://dx.doi.org/10.1107/S0365110X56002382>
- Xue D, Kitamura K (2002). Dielectric characterization of the defect concentration in lithium niobate single crystals. *Solid State Commun* 122:537–541.[http://dx.doi.org/10.1016/S0038-1098\(02\)00180-1](http://dx.doi.org/10.1016/S0038-1098(02)00180-1)
- Yang CS, Liu Q, Kauzlarich SM (2000). Synthesis and characterization of Sn/R, Sn/Si-R, and Sn/SiO₂ core/shell nanoparticles. *Chem. Mater.* 12:983 <http://dx.doi.org/10.1021/cm990529z>
- Zhang P, Gao L (2003). Synthesis and Characterization of CdS Nanorods via Hydrothermal Microemulsion. *Langmuir* 19:208 <http://dx.doi.org/10.1021/la0206458>